Colloids and Surfaces A: Physicochemical and Engineering Aspects 682 (2024) 132965

Contents lists available at ScienceDirect

Colloids and Surfaces A: Physicochemical and Engineering Aspects

journal homepage: www.elsevier.com/locate/colsurfa

3D printing of magnetically responsive superhydrophobic porous membranes with on-demand oil-absorption property

Shuyi Li [a], Zhengyi Song [a,*], Yuyan Fan [c], Dongsong Wei [a], Chenchen Liao [a], Chengyu Du [a], Xiaoxia Yan [d], Zhiwu Han [a], Yan Liu [a,b,**]

[a] Key Laboratory of Bionic Engineering (Ministry of Education), Jilin University, Changchun 130022, China
[b] Institute of Structured and Architected Materials, Liaoning Academy of Materials, Shenyang 110167, China
[c] National Key Laboratory of Science and Technology on Micro/Nano Fabrication, Shanghai Jiao Tong University, Shanghai 200240, China
[d] College of Food Science and Engineering, Jilin University, Changchun 130022, China

GRAPHICAL ABSTRACT

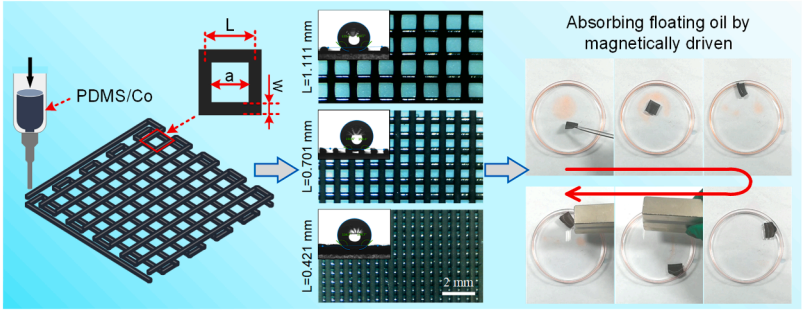

ARTICLE INFO

Keywords:
Direct ink writing
Magnetically responsive
Porous membranes
Superwettability
Oil-absorption

ABSTRACT

The preparation of superhydrophobic porous materials using 3D printing technology has attracted extensive attention in numerous fields. Herein, a magnetically active PDMS/cobalt powder (PDMS/Co) porous membrane with superwettability was prepared by direct ink writing (DIW) 3D printing. The structural parameters of the porous membrane with different Co powder contents were adjusted by controlling printing parameters, such as printing speed, air pressure and filament spacing, and the variation range of the structural parameters enabling the porous membranes exhibit superhydrophobic properties was finally determined. Owing to the magnetic activity of the Co powder, remotely directional collection of floating oil in water was achieved by manipulating a permanent magnet. In addition, the chemical stability and mechanical stability of the porous membrane were investigated. The method presented here is expected to be applied to remote control of oil adsorption, providing a new strategy for solving the pollution problem caused by oily wastewater.

* Corresponding author.
** Corresponding author at: Key Laboratory of Bionic Engineering (Ministry of Education), Jilin University, Changchun 130022, China.
E-mail addresses: zysong@jlu.edu.cn (Z. Song), lyyw@jlu.edu.cn (Y. Liu).

https://doi.org/10.1016/j.colsurfa.2023.132965
Received 27 September 2023; Received in revised form 3 December 2023; Accepted 8 December 2023
Available online 10 December 2023

1. Introduction

Superwetting surfaces in nature have inspired the creation of a large number of biomimetic materials with superwetting properties, which have a wide range of applications in numerous industries [1–3]. Among them, superhydrophobic/ superoleophilic materials are a class of materials that are extremely repellent to water but prefer to absorb oil, usually consisting of special surface micro- and nano-roughness structures and low surface energy chemicals [4,5]. Noteworthy, porous materials with superwetting properties have an important application in the field of water filtration and selective oil/water separation because of their advantages such as low density, high porosity and high oil absorption [6–9]. However, the current preparation methods for superhydrophobic porous materials typically require an additional process, i.e., the construction of a new coating with micro-nanostructures on the pristine surface of the porous material, such as spraying [10], chemical/laser/plasma etching [11,12], electrodeposition [13,14], and dipping [15,16]. The preparation process of these methods is relatively complicated, and the prepared materials are prone to lose the original superhydrophobic properties due to the damage of the micro-nanostructures on the surface.

As an emerging technique, 3D printing, also called as additive manufacturing, has the significant advantages of rapid and precise prototyping, which can be used to help mimicking bionic structures and produce various complex architectures [17–20]. Importantly, 3D printing technology allows for on-demand customization of pore sizes, providing tremendous flexibility in the fabrication of superhydrophobic porous structures [21,22]. For printing methods that can reach micro- and nano-levels of precision, such as two-photon polymerisation, it is possible to directly build the printed material into superhydrophobic porous structures with micro- and nano-structures [23–26]. Whereas, for other 3D printing methods, i.e., Fused Deposition Modeling (FDM), Direct Ink Writing (DIW), Digital Light Projection (DLP), etc., it is feasible to attach coatings on pre-printed porous structures through post-processing, but there are still issues with the uniformity and damage resistance of the coatings [27–31]. In contrast, by uniformly mixing nanoparticles in a matrix system with low surface energy, porous structures and surface micro-nano-structures can be simultaneously constructed during the printing process, which simplifies the tediousness of the manufacturing process for surface wettability [32,33]. 3D-printed superhydrophobic porous structures without post-processing have demonstrated manoeuvrability in water treatment and oil-water separation applications [34–36]. Unfortunately, superhydrophobic porous structures fabricated by 3D printing do not yet have stimulus-responsive properties, meaning that porous membranes cannot be manipulated remotely.

Herein, we prepared super-wetting PDMS/cobalt powder (PDMS/Co) porous membranes consisting of vertically interlaced filaments with magnetically responsive properties using pneumatic assisted DIW 3D printing technology. By programming the printing parameters, such as printing speed, printing air pressure and filament spacing, the structural parameters of porous membranes with different Co powder contents can be modulated without the need for other physical or chemical treatments, thereby manipulating the surface wetting properties to achieve the superhydrophobic behaviour without the need of any other physical or chemical treatments. Afterwards, the chemical and mechanical stability of the superhydrophobic properties of the porous membrane were verified. In addition, owing to the magnetic activity conferred by the incorporation of Co powder, the directional collection of floating oil was achieved by manipulating the movement of the porous membranes in the oil-water mixture through a remote magnetic field.

2. Experimental

2.1. Materials

The polydimethylsiloxane (PDMS, SE1700) base elastomer and curing agent were purchased from Dow Corning Corporation, USA. Co powder was provided by Hebei Robo Metal Material Technology Co., Ltd. (China), with diameter of approximately 2–4 μm. Petroleum ether, n-hexane and toluene were provided by Guomao Group Chemical Reagent Co., Ltd. Petrol and vacuum pupm oil was obtained from local market.

2.2. Ink preparation

Firstly, 10 g of PDMS and 1 g curing agent were pre-mixed in a beaker. Subsequently, different amount Co power was added into the previous beaker, and mechanically stirred for 10 min under ice bath conditions. Among that, the X:1 was used to distinguish ink formula, i.e, PDMS: Co powder=X:1, X represented the mass ratio of PDMS in each formula system. Then, the printing ink was transferred to the syringe, centrifuging at 1200 r/min for 10 min to remove air bubbles, which should be prepared fresh and used at room temperature.

2.3. 3D printing of PDMS/Co porous membranes

In this study, a homemade pneumatic assisted direct ink writing (DIW) 3D printer with a computer-controlled X-Y-Z axis movement platform was used to print PDMS/Co porous membranes. The typical 3D printing process was consisting of building a three-dimensional model, slicing, generating G code and extrusion deposition. The slicing process performed using the open-source software *slic3r* programmed the printing speed, printing path and layer thickness, etc. As shown in Fig. 1, according to the set printing parameters, the micro-nozzle with an inner diameter of 310 μm moved along the X and Y axes and extruded the ink onto the glass substrates, forming the pre-designed patterns. During the printing process, before printing the filaments in the Y-axis direction to form the next layer, the micro-nozzle was lifted up by 0.24 mm along the Z axis. As a result, the ordered porous membranes were composed of 2–4 vertically staggered layers of materials, with a thickness of 0.4–0.8 mm. Among that,

$$a=L-w$$

In which, a is the side length of the printed pores. L is the filament spacing, controlled by changing the filling ratio in the slice setting. The filling rate set in this research ranged from 25% to 80%, and the corresponding filament spacing was as shown in Table 1. *w* is the filament width, controlled by the coordinated configuration of two parameter variables, printing speed and air pressure. The variable range of air pressure was from 400 KPa to 700 KPa, and the speed varied from 1 mm/s to 6 mm/s.

Finally, the printed PDMS/Co porous membranes were peeled off from the glass substrate after curing at 95 °C for 2 h, reserved for the next tests and characterization.

2.4. Rheological measurement

The RSO Oscillatory Rheometer (AMETEK Brookfield, USA) was used to characterize the rheological properties of as-prepared inks in different proportions, which were performed at a temperature of 25 °C (Peltier temperature control). The relationship between the viscosity and shear rate for different inks were analyzed at a shear rate range of 0.1–100 s^{-1}. Moreover, the oscillation sweep experiment was to perform an amplitude sweep test under a frequency of 1 Hz and an oscillatory stress range of 10–10000 Pa, so as to observe the changes in the storage modulus (G') and loss modulus (G") of the inks.

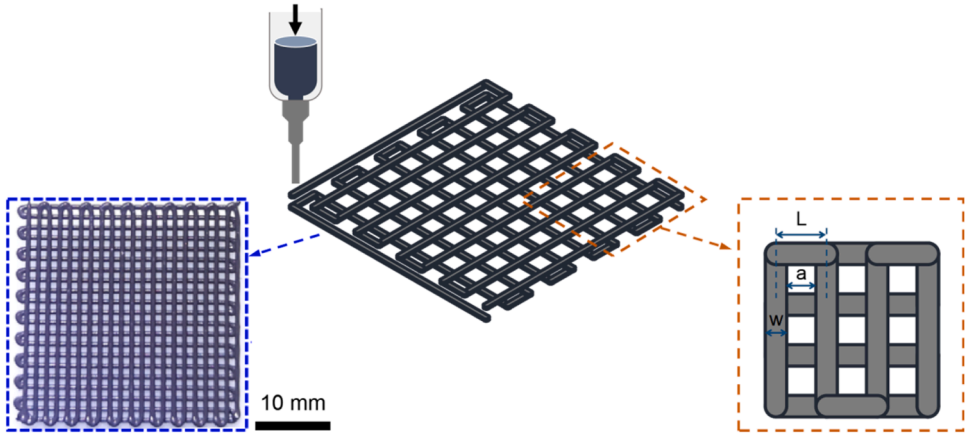

Fig. 1. The schematic diagram of 3D printing process of superwetting PDMS/Co porous membrane. The left is an optical image of the printed PDMS/Co porous membrane.

Table 1
Correspondence between filament spacing and filling rate.

Filling rate (%)	25	26.5	29	32	36	42	50	60	70	80
Filament spacing (mm)	1.278	1.111	1.015	0.921	0.818	0.701	0.589	0.491	0.421	0.368

2.5. Characterization

The scanning electron microscope (SEM, EVO18, ZEISS) and laser confocal scanning microscope (LCSM, OLS3000) were used to measure the surface morphologies. The surface wettability of the specimens was evaluated via a contact angle meter (Kruss DSA25S, Germany). The water contact angles (WCAs) were performed for at least three times at different locations of the specimen. The Fourier-transform infrared spectrophotometer (FTIR, JASCO, Japan) was used to characterize the chemical component. The magnetic properties of porous membranes were measured using a Tesla meter (TD8620).

2.6. Oil or solvent adsorption capacity tests

The adsorption property of samples was measured by weighing the porous membranes before and after the absorption of oil or organic solvent, which was according to the following equation:

$$q = (m - m_0)/m_0$$

where q was the capacity of the porous membrane; m and m_0 were the weight of the porous membranes after and before the oil adsorption, respectively.

3. Results and discussion

3.1. Rheological property

The rheological behavior of PDMS inks with different Co powder content and the effects on the printed results were shown in Fig. 2. The pure SE 1700 PDMS presented the rheological properties of a non-Newtonian fluid and could be directly used for DIW 3D printing (Fig. 2**a**). When added the hydrophobized Co powder in pure PDMS, i.e., 8:1, 5:1 or 2:1, along with the increasing content, the viscosity of ink gradually increased under the same shear rate. Meanwhile, with the acceleration of the shear rate, the inks with different proportions of Co powder showed the nature of shear thinning, indicating that the formulated inks were a pseudo-plastic fluid, which were suitable for material extrusion 3D printing. Although the change in the content of Co

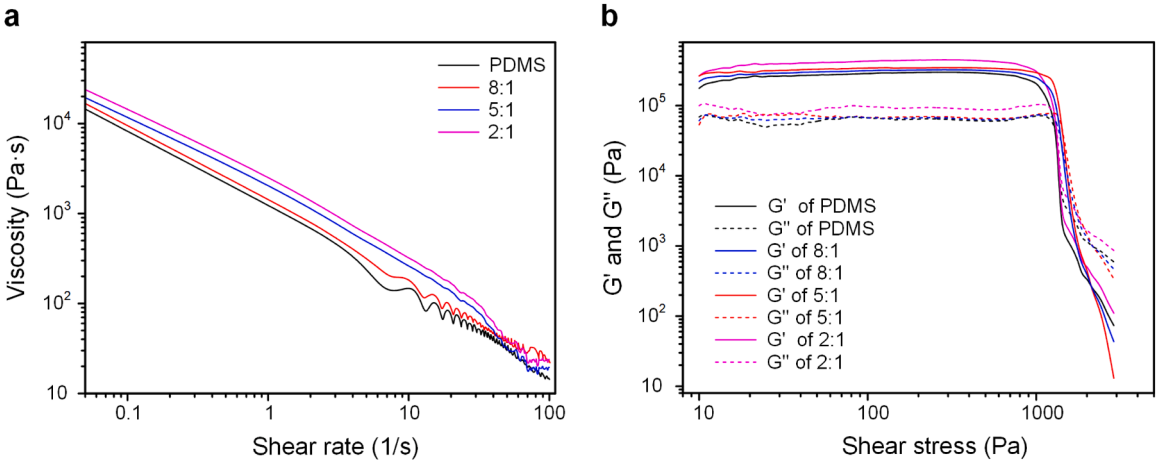

Fig. 2. Rheological properties and printability of PDMS/Co inks. (a) Apparent viscosities of four inks with different Co power as a function of shear rate. (b) The storage modulus (G′) and loss (G′′) modulus of four inks as a function of shear stress.

powder changed the viscosity of the ink, the shear thinning behavior didn't change significantly. Afterwards, the effects of the addition of Co powder on the printing performance will be analyzed in the next.

Meanwhile, the oscillatory shear test in Fig. 2**b** was implemented to assess the shape retention ability of the Co/PDMS inks in the 3D printing process. No matter the pure PDMS or loading the various Co powder, the storage modulus (G′) of inks were all over 10^5 Pa, which was more than loss modulus (G'') in the low shear stress region. Moreover, with the increase of Co powder content, the storage modulus and loss modulus were increased compared with pure PDMS. It showed that the addition of Co powder further improved the shape retention of the material, which was beneficial to the extrusion of ink. In addition, with the increase of shear stress, both the storage modulus and the loss modulus showed a decreasing trend. The faster drop in storage modulus allowed the two curves to intersect, indicating a gradual increase in the fluidity of the materials. Hence, the prepared ink had the properties of a gel, which presented a viscoelastic solid state.

3.2. Design and fabrication of the porous membrane surface

The setting of printing parameters will have an influence on the extrusion of filament, including printing speed and air pressure, so as to affect the wettability of porous PDMS/Co membrane. Therefore, we investigated the relationship between the width of the extruded filament with different Co powder content and the printing speed under different air pressure conditions, which were shown in Fig. 3**a-d**. It can be concluded that higher air pressure or slower speed can result in an increase in the filament width. Moreover, with the increase of Co powder content, the width of the extruded line gradually decreased under the same air pressure and speed. This is because the addition of Co powder increased the viscosity of the ink, and the total volume of the extruded material per unit time decreased accordingly. As a result, the filament width showed a decreasing trend. In order to facilitate the investigation of the influence of pore size on the hydrophobic properties of the porous membranes, it is necessary to ensure that the filament widths of different inks are as consistent as possible. Therefore, we selected four sets of parameters with the filament width around 0.4 mm, which were marked in the Fig. 3**a-d**, namely pure PDMS (500 KPa, 4 mm/s), 8:1 (500 KPa, 3 mm/s), 5: 1 (500 KPa, 3 mm/s) and 2:1 (600 KPa, 3 mm/s), respectively.

Meanwhile, due to the importance of porous structures in surface superwetting performance, the influences of the pore size on the wettability changes of membrane surface were discussed. For PDMS inks with different Co powder contents, porous membrane surface specimens with different pore sizes were 3D printed by adjusting the filling rate ranging from 25% to 80%, so as to resulting in the corresponding variation of filament spacing from 0.3 to 1.3 mm. As can be seen from Fig. 4, the pores formed by the vertical filaments of the upper and lower layers of materials exhibited a square shape. With the gradual increase of the filling rate, the filament spacing became significantly smaller, and the side length of the square hole also gradually decreased, which was a linear regression relation. At 70% filling rate, the pores tend to disappear and disappeared at 80% filling rate (as shown in Fig. 4). While the printed filament was fixed, the filament spacing could affect the side length of square pore. The statistical results showed that the side length of square pore of all porous membranes increased with the increasing of

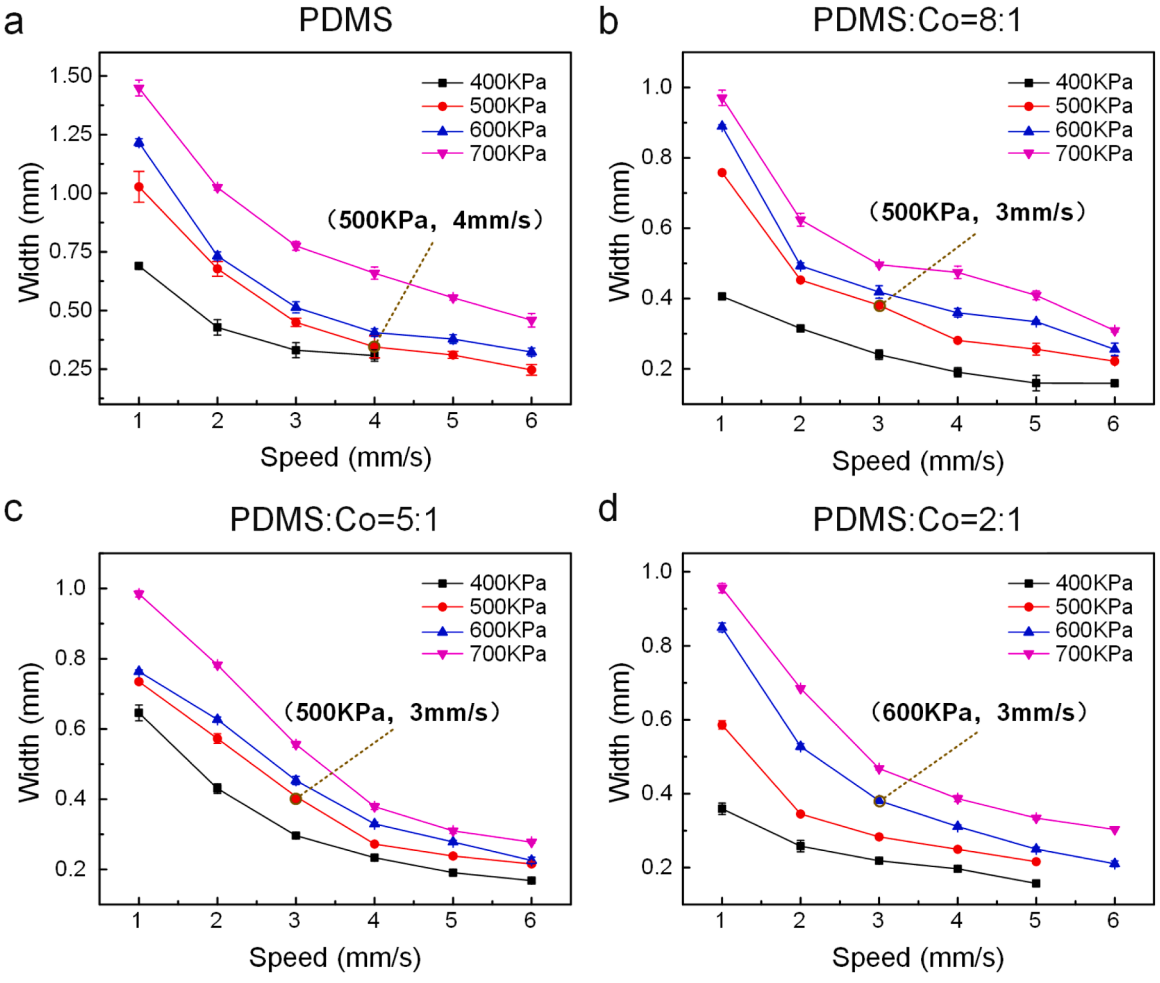

Fig. 3. The relationship of printing speed and air pressure on the filaments for different inks, (a) pure PDMS, (b) 8:1, (c) 5:1, (d) 2:1.

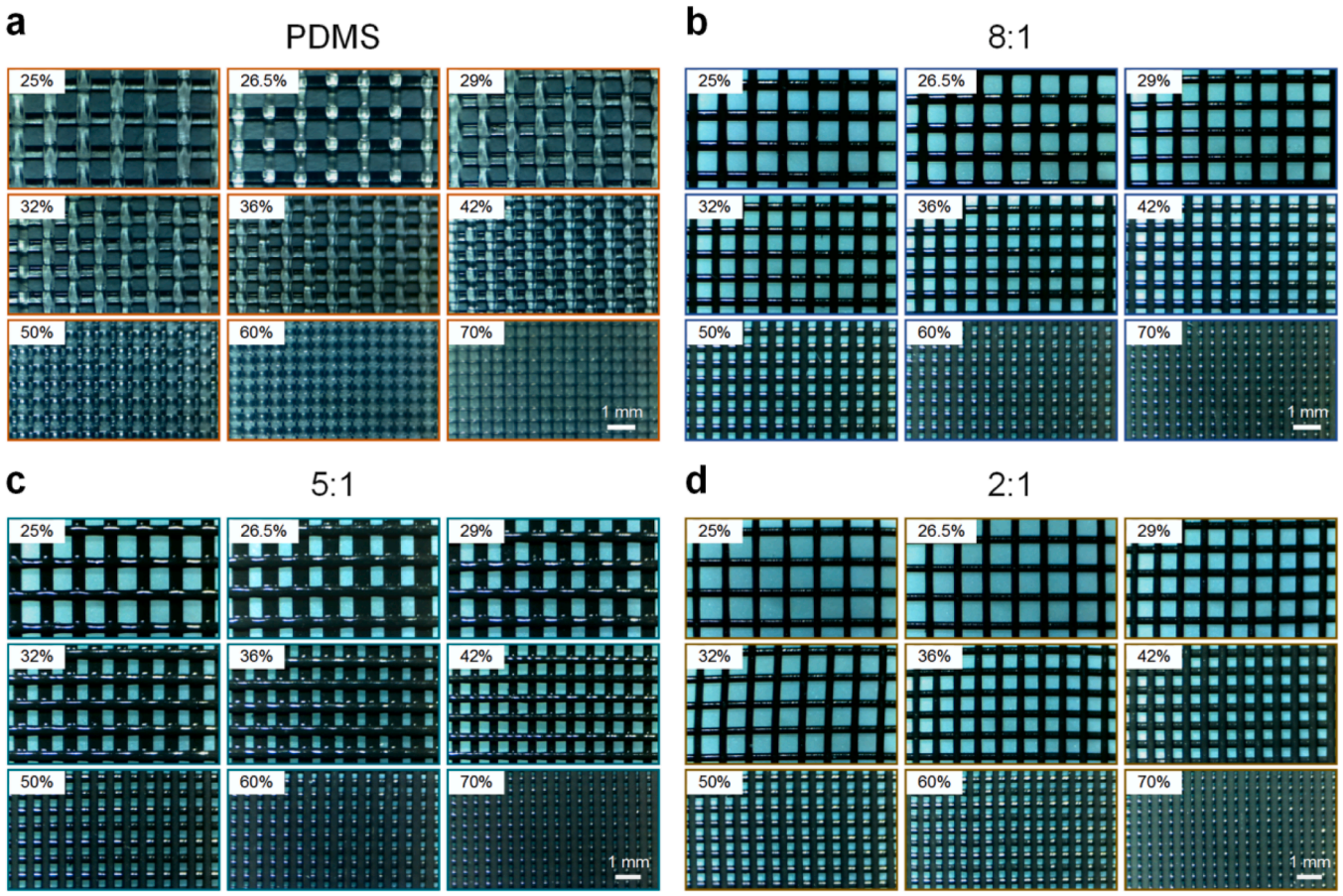

Fig. 4. The optical microscope images of porous membranes printed with different inks under the different filling rates, (a) pure PDMS, (b) 8:1, (c) 5:1, (d) 2:1.

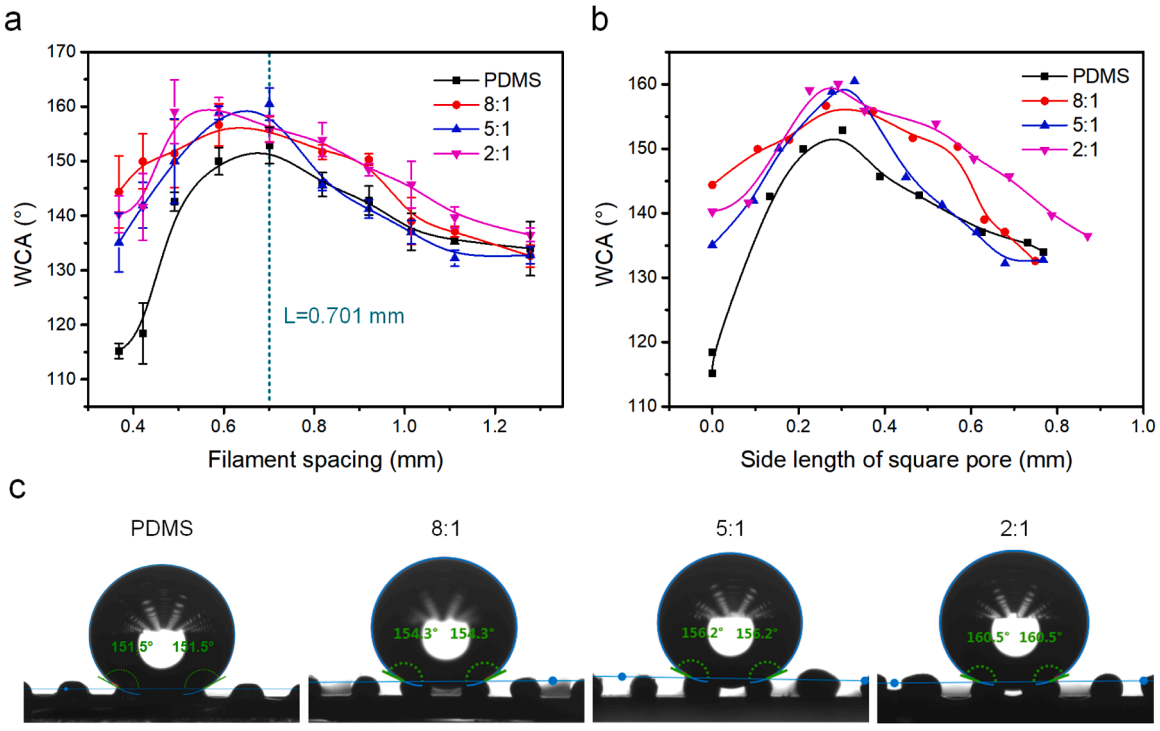

Fig. 5. WCA testing of porous membranes. Relationship between WCAs of porous membranes and filament spacing (a) and pore size (b). (c) Images of WCAs of different porous membranes with a filament spacing of 0.701 mm.

filament spacing, which was a linear regression relation (as shown in Fig. S1). Because of the effect of ink collapse, the pores of PDMS/Co membranes (8:1, 5:1, or 2:1) were also bigger than the pure PDMS membrane at the similar filament spacing, thus affecting the surface wettability, which will be discussed in the next.

3.3. Wettability property

The wettability of all porous membranes in Fig. 4 were investigated to probe the correlation between WCAs and structural parameters of the pores. As shown in Fig. 5, for the pure PDMS material with lower surface energy (the intrinsic contact angle of 106°), the values of WCAs can also be significantly increased by configuring it into porous structures with different pore sizes via DIW 3D printing. While with printed filament of 0.701 mm and side width of 0.302 mm, the pure PDMS membrane surface exhibited superhydrophobic property with a WCA of exceeding 150°, indicating that the gridded structural treatment had a certain effect on the roughness of the membrane surface. Therefore, the material property of low surface energy and rough structure endowed the porous PDMS membrane with superhydrophobicity.

Along with the increase of addition content of Co powder, the hydrophobicity of porous PDMS/Co membranes had been enhanced to some extent (Fig. 5a, b). Fig. 5c showed the WCA measurements of four different superhydrophobic membranes with a filament spacing of 0.701 mm as follows, 151.5°, 154.3°, 156.2° and 160.5°. Specifically, as for the addition content of 8:1, the porous membrane exhibited superhydrophobic property while the filaments and the side lengths are in the range of 0.491–0.921 mm and 0.178–0.569 mm, respectively. As the addition of Co powder increased to 5:1, the filaments within range of 0.491–0.701 mm and the side lengths of 0.154–0.330 mm could achieve the superhydrophobic membranes. While the Co powder content up to 2:1, the filaments of the porous membrane with superhydrophobic property are in the range of 0.491–0.818 mm, and the corresponding pore side length were 0.225–0.519 mm. Hence, it can be concluded that, for 3D printed PDMS/Co porous membranes, the pore side length required to achieve superhydrophobic property was between 0.2 and 0.6 mm. Therefore, when performing the subsequent performance analysis of the porous membrane, the side length of the pores of the printed filament was set in the range of 0.3–0.5 mm, and the corresponding filament spacing was in the range of 0.5–0.9 mm. In addition, the WCA values of porous membranes with different contents of Co powder all showed a trend of firstly increasing and then decreasing with the increase of filament spacing or side length of pore. Therefore, the results proved that both the filament spacing and ink property could affect the wettability of the porous membrane.

3.4. Morphology analysis

The characterization of the microscopic morphology is favorable to reveal the superhydrophobic mechanism of flexible PDMS/Co porous membranes. The results of optical microscope demonstrated that, the printed porous membranes exhibited a smooth and flat state (Fig. 6**a**). However, according to the further investigation by SEM images in Fig. 6**c-f**, expect for the pure PDMS porous membrane surface, the micron particles in the surface exhibited a gradual increase with the addition of Co powder. However, since the vast majority of Co powders were wrapped by PDMS colloids, the surface morphologies didn't show an obvious micro-nano hierarchical microstructure. Furthermore, combined with the investigation of laser confocal scanning microscope (Fig. S2), the surface roughness values (Ra) of pure PDMS, PDMS/Co (8:1, 5:1 and 2:1) were 3.243 μm, 17.948 μm, 21.085 μm and 30.571 μm, respectively. Meanwhile, based on the FTIR results in Fig. 6**b**, the obvious characteristic peak at 2964 cm^{-1} was ascribed to the stretching vibration of C-H in -CH_3, and the characteristic peaks at 1007.6 and 786.3 cm^{-1} were resulted from Si-O-Si group, which are the main functional groups of PDMS and also belong to the hydrophobic functional groups.

Based on the above results, it indicated that DIW 3D printing could effectively control the formation of the roughness of the membrane surface by combining inks with different filler contents with the adjustment of the pore size of the porous membrane, thereby influencing the wettability. Following the principles of high efficiency and economy, the PDMS/Co ink with 5:1 radio was selected in the follow-up, along with an air pressure of 500 KPa, a printing speed of 3 mm/s, and a printing filling rate of 50%, so as to carry out the performance and application research of porous membranes.

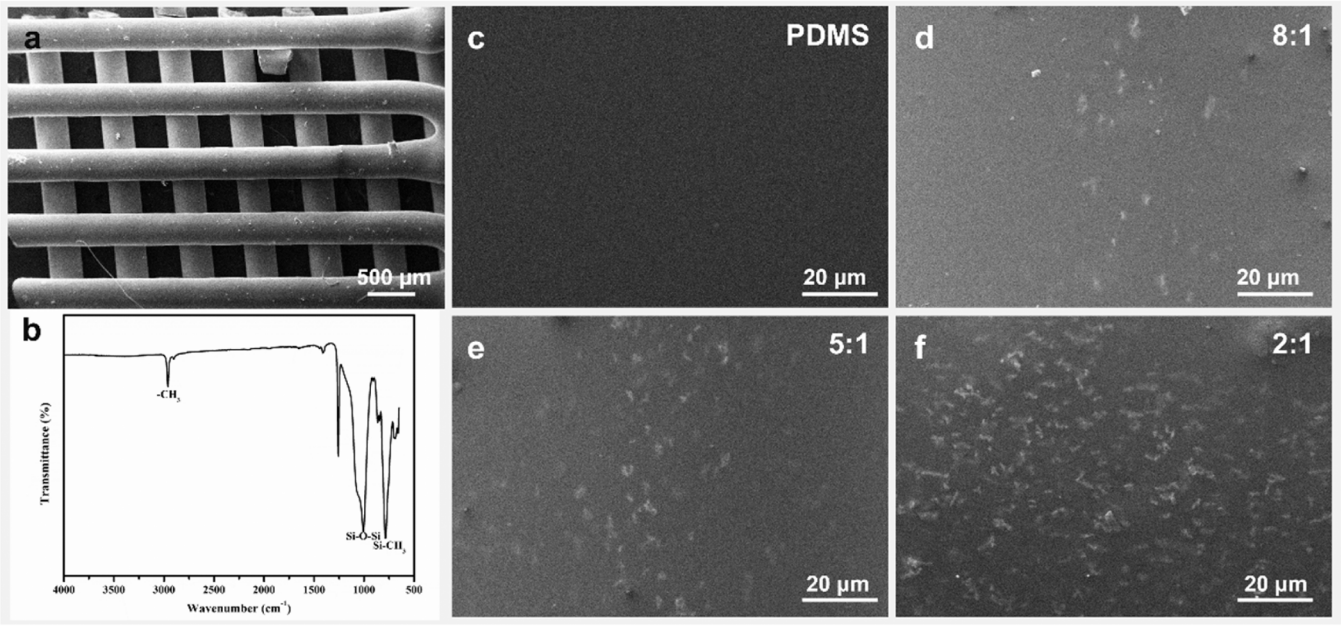

Fig. 6. The SEM image (a) and FT-IR spectra (b) of the surface of printed porous membrane. And the magnifying SEM images porous membrane surface of different inks, (c) pure PDMS, (d) 8:1, (e) 5:1, (f) 2:1.

3.5. Stability

Surface stability is the key to determining the use value of materials. As a flexible elastomer, the porous PDMS membrane has good mechanical stability. As shown in Fig. 7**a and b**, the printed superhydrophobic PDMS/Co membrane was tested by multiple stretching and bending deformations. Even though with more than 600 times of stretching-releasing cycles with a strain of 50% and multiple irregular folding, the WCA values of the printed membrane remained above 150°. The results demonstrated the printed superhydrophobic membrane has good elasticity and excellent mechanical stability, should be attributed not only to the conformability of the flexible matrix material, but also the advantage of 3D printing technology, which directly transformed PDMS/Co ink into superhydrophobic surfaces with a porous structure. By comparison with traditional coating method, this method can effectively solve the weak interfacial adhesion between the two materials and avoid the detachment of Co particles from the surface during force-induced deformation. In addition, for the solutions with different pH values shown in Fig. 7**c**, no matter acid or alkaline solution, the WCA values of the printed PDMS/Co porous membrane also were greater than 150°, showing superhydrophobic property. Moreover, the porous membrane can maintain superhydrophobicity for a period of time in air (Fig. 7**d**).

3.6. Magnetic response on-demand oil-absorption

In view of the hydrophobic and oil absorption properties of PDMS, the oil absorption capacity of the 3D printed porous membrane also was investigated. As shown in Fig. 8**a**, while pure PDMS was immersed in petroleum ether solution, the volume expanded in a linear expansion rate of about 35%. As for the printed PDMS/Co porous membrane with 5:1 content (filament spacing was about 0.59 mm), it also exhibited oil-absorbing swelling capacity with a similar linear expansion rate. In addition, we have conducted tests on the adsorption capacity of the two membranes for different types of solvents and oils. As shown in Fig. 8b, the PDMS and PDMS/Co membranes exhibited different oil-adsorption capacities depending on the density of the adsorbed oil. Overall, due to the addition of Co powder, the adsorption capacity of PDMS/Co membranes has decreased compared to PDMS membranes, but they still possess considerable oil adsorption performance. Specifically, for high-density oils such as vacuum pump oil and petrol, the adsorption capacity of the two membranes was less than 100 g/g. As for low-density solvents such as n-hexane, toluene, and petroleum ether, the adsorption capacity of PDMS membrane ranged from 142.4 g/g to 172.9 g/g, whereas the adsorption capacities of the PDMS/Co membranes decreased, with values ranging from 82.4 g/g to 109.1 g/g. Moreover, the presence of Co powder endows the PDMS/Co porous membrane with magnetically responsive properties of 0.03–0.05 mT (8:1), 0.09–0.11 mT (5:1), and 0.15–0.17 mT (2:1) as measured by a Tesla meter, which allows the porous membrane to produce controlled motion in response to the magnetic field. Utilizing the dual characteristics of the oil absorption and magnetic response of PDMS/Co porous membranes, the adsorption and collection of oil in the oil-water mixture can be realized concurrently. As shown in Fig. 8**c,** the movement of the porous membrane can be controlled by manually manipulating the position of an external magnet to achieve directional collection of floating oil in water, with

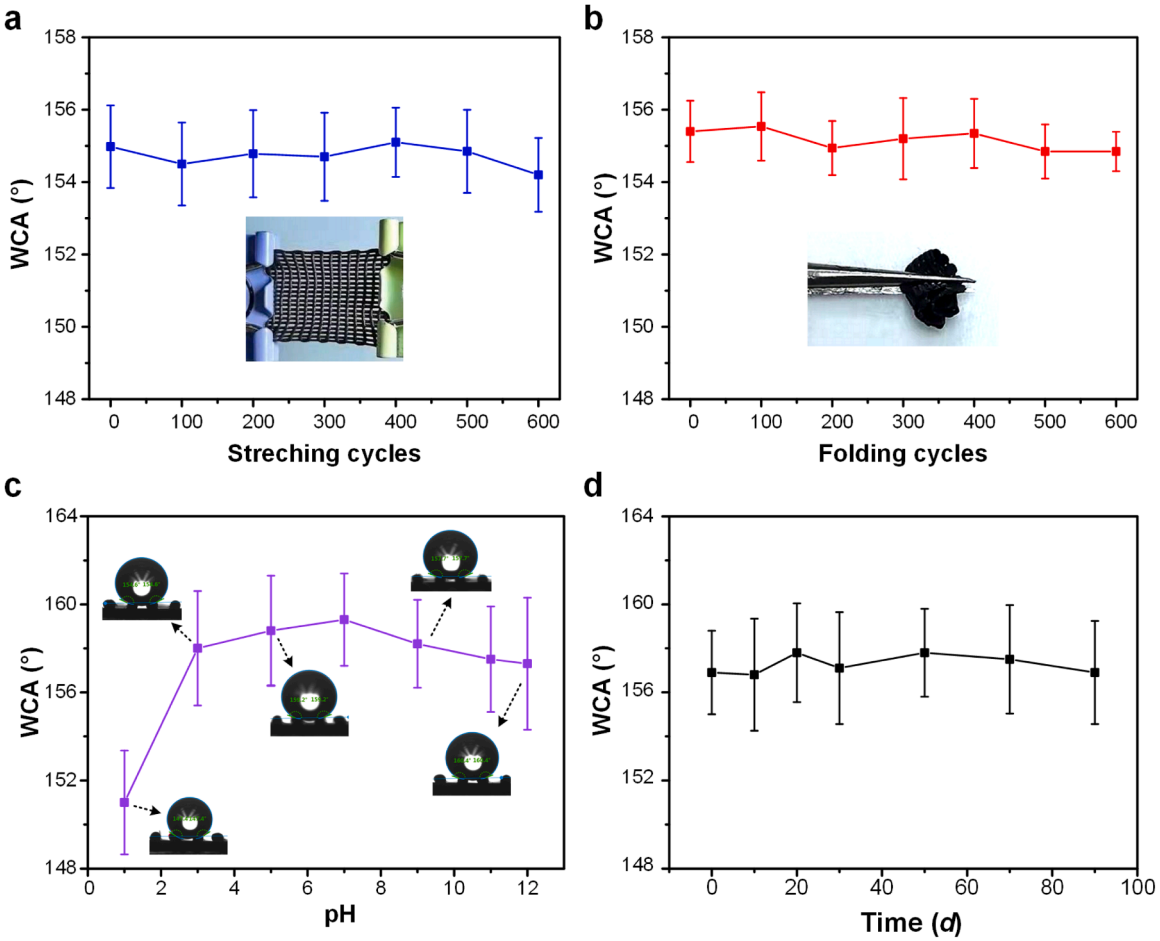

Fig. 7. Stability test of WCA of porous membranes. (a) Multiple elastic stretching-releasing cycles. (b) Multiple irregular folding. (c)Plots of WCA of porous membranes at different pH solutions. (d) Long-term stability tests in air.

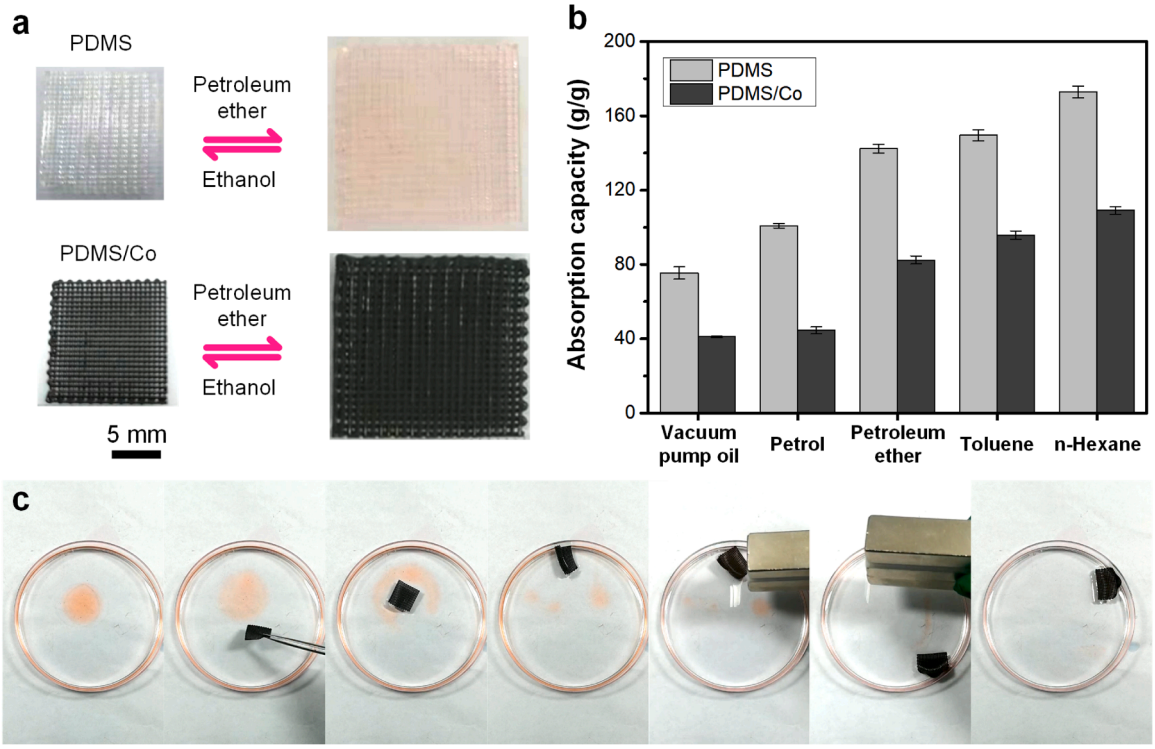

Fig. 8. The adsorption test of PDMS and PDMS/Co porous membranes with 5:1 content. (a) Images of the PDMS and PDMS/Co membranes before and after absorbing petroleum ether. (b) Adsorption capacity of the PDMS and PDMS/Co membranes for various solvents and oils. (c) Directional collection of floating oil in water in response to magnetic field.

non-contact and remote oil absorption characteristics. Moreover, after cleaning with alcohol, the PDMS/Co membrane could quickly return to the initial state, achieving the use of recycled.

4. Conclusion

Via a facile and environment-friendly approach, we prepared superwetting PDMS/Co porous membranes with on-demand oil-absorption property utilizing pneumatic assisted DIW 3D printing technology. By adjusting printing parameters such as ink ratio, printing speed, air pressure and filament spacing, the structural porous membranes with superhydrophobicity could be obtained easily without further physical or chemical treatment. For low surface energy materials of PDMS, the filament spacing and the amount of Co powder added jointly affected the wettability of the porous membranes. Especially, the pore size of porous membranes can be adjusted and designed via parameter settings. The results demonstrated that the pore size ranges from 0.2 to 0.6 mm to achieve superhydrophobicity. In addition, the porous membranes exhibited excellent chemical stability and mechanical stability. Owing to the magnetic activity of the Co powder, remotely directional collection of floating oil in water was achieved by manipulating a permanent magnet. This provides a novel and high degree of freedom for the preparation technology of superhydrophobic surface, which could have a wide range of potential applications.

CRediT authorship contribution statement

Liao Chenchen: Conceptualization, Investigation. **Fan Yuyan:** Data curation, Methodology. **Wei Dongsong:** Methodology. **Li Shuyi:** Conceptualization, Funding acquisition, Investigation, Methodology, Writing – original draft, Writing – review & editing. **song Zhengyi:** Data curation, Funding acquisition, Methodology, Writing – review & editing. **Han Zhiwu:** Funding acquisition, Resources. **Liu Yan:** Funding acquisition, Resources, Supervision. **Du Chengyu:** Investigation. **Yan Xiaoxia:** Conceptualization, Methodology.

Declaration of Competing Interest

The authors declare that they have no known competing financial interests or personal relationships that could have appeared to influence the work reported in this paper.

Data availability

Data will be made available on request.

Acknowledgement

The authors thank the National Natural Science Foundation of China (No. 52105297, U22A20183), Innovative Research Groups of the National Natural Science Foundation of China (No.52021003), Science and Technology Development Project of Jilin Province (20210508029RQ), Scientific Research Project of Jilin Provincial Department of Education (JJKH20231152KJ) and JLU Science and Technology Innovative Research Team (No. 2020TD-03).

Appendix A. Supporting information

Supplementary data associated with this article can be found in the online version at doi:10.1016/j.colsurfa.2023.132965.

References

[1] Y.R. Wei, F.Y. Wang, Z.G. Guo, Bio-inspired and metal-derived superwetting surfaces: function, stability and applications, Adv. Colloid Interfac. 18 (2023), 102879.
[2] T.A. Otitoju, A.L. Ahmad, B.S. Ooi, Superhydrophilic (superwetting) surfaces: a review on fabrication and application, J. Ind. Eng. Chem. 47 (2017) 19–40.

[3] M.Z. Khan, J. Militky, M. Petru, B. Tomkova, A. Ali, E. Toren, S. Perveen, Recent advances in superhydrophobic surfaces for practical applications: a review, Eur. Polym. J. 178 (2022), 111481.
[4] S. Rasouli, N. Rezaei, H. Hamedi, S. Zendehboudi, X.L. Duan, Superhydrophobic and superoleophilic membranes for oil-water separation application: a comprehensive review, Mater. Des. 204 (2021), 109599.
[5] J. Usman, M.H.D. Othman, A.F. Ismail, M.A. Rahman, J. Jaafar, Y.O. Raji, A. O. Gbadamosi, T.H. El Badawy, K.A.M. Said, An overview of superhydrophobic ceramic membrane surface modification for oil-water separation, J. Mater. Res. Technol. 12 (2021) 643–667.
[6] Y.P. Song, J. Phipps, C.J. Zhu, S.Q. Ma, Porous materials for water purification, Angew. Chem. Int. Ed. 62 (11) (2023), e202216724.
[7] L. Kang, L.J. Shi, L.F. Song, X.P. Guo, Facile fabrication of superhydrophobic porous materials using the water-based aza-Michael reaction for high-efficiency oil-water separation, Sep. Purif. Technol. 308 (2023), 122880.
[8] Z.P. Fang, Z.M. Guo, Y.Y. Fan, S.Y. Li, Z.W. Han, Y. Liu, Large-scale preparation of a versatile bioinspired sponge with physic-mechanochemical Robustness for multitasking separation, J. Hazard. Mater. 435 (2022), 128902.
[9] U. Baig, M. Faizan, A. Waheed, A review on super-wettable porous membranes and materials based on bio-polymeric chitosan for oil-water separation, Adv. Colloid Interf. 303 (2022), 102635.
[10] F. Wang, R.R. Ma, J.L. Zhan, W.S. Shi, Y.Y. Zhu, Y.Q. Tian, Superhydrophobic/superoleophilic starch-based cryogels coated by silylated porous starch/Fe_3O_4 hybrid micro/nanoparticles for removing discrete oil patches from water, Sep. Purif. Technol. 291 (2022), 120872.
[11] T.A. Saleh, N. Baig, Efficient chemical etching procedure for the generation of superhydrophobic surfaces for separation of oil from water, Prog. Org. Coat. 133 (2019) 27–32.
[12] J.L. Yong, Q. Yang, C.L. Guo, F. Chen, X. Hou, A review of femtosecond laser-structured superhydrophobic or underwater superoleophobic porous surfaces/materials for efficient oil/water separation, RSC Adv. 9 (22) (2019) 12470–12495.
[13] J.J. Xuan, L.K. Xu, Y.L. Xin, L.L. Xue, L. Li, Robust superhydrophobic Ni-Co electrodeposited carbon felt for hot water repellency and controllable oil/water separation, J. Environ. Chem. Eng. 11 (1) (2023), 109102.
[14] N. Xu, X.Y. Yu, S.H. Yu, Y.Y. Han, T.X. Zhang, H.Q. Chu, Characterization of electrodeposited porous structured composite layers and their unconventional wettability properties, Colloid Surf. A 654 (2022), 130074.
[15] C.Y. Cao, J. Cheng, Fabrication of superhydrophobic copper stearate@ Fe_3O_4 coating on stainless steel meshes by dip-coating for oil/water separation, Surf. Coat. Tech. 349 (2018) 296–302.
[16] C.L. Xu, Y.T. Luo, L. Zhou, Y.W. Bi, H. Sun, Fabrication of durable superhydrophobic stainless steel mesh with nano/micro flower-like morphologies for self-cleaning and efficient oil/water separation, J. Bionic Eng. 19 (6) (2022) 1615–1624.
[17] S.H. Siddique, P.J. Hazell, H.X. Wang, J.P. Escobedo, A.A.H. Ameri, Lessons from nature: 3D printed bio-inspired porous structures for impact energy absorption-A review, Addit. Manuf. 58 (2022), 103051.
[18] S. Yu, Y.H. Hwang, K.T. Lee, S.O. Kim, J.Y. Hwang, S.H. Hong, Outstanding strengthening and toughening behavior of 3D-printed fiber-reinforced composites designed by biomimetic interfacial heterogeneity, Adv. Sci. 9 (3) (2022), 2103561.
[19] Y. Yang, X. Song, X.J. Li, Z.Y. Chen, C. Zhou, Q.F. Zhou, Y. Chen, Recent progress in biomimetic additive manufacturing technology: From materials to functional structures, Adv. Mater. 30 (36) (2018), 1706539.
[20] C.Y. Yan, P. Jiang, X. Jia, X.L. Wang, 3D printing of bioinspired textured surfaces with superamphiphobicity, Nanoscale 12 (5) (2020) 2924–2938.
[21] H.S. Liu, Z.P. Zhang, C.Y. Wu, K. Su, X.A. Kan, Biomimetic superhydrophobic materials through 3D printing: progress and challenges, Micromachines 14 (6) (2023) 1216.
[22] H. Sun, W. Tian, Y.X. Sun, M.J. Li, 3D-printed mesh membranes with controllable wetting state for directional droplet transportation, Colloid Surf. A 638 (2022), 128143.
[23] Y. Yang, X.J. Li, X. Zheng, Z.Y. Chen, Q.F. Zhou, Y. Chen, 3D-printed biomimetic super-hydrophobic structure for microdroplet manipulation and oil/water separation, Adv. Mater. 30 (9) (2018), 1704912.
[24] B.C. Wang, J. Chen, C. Kowall, L. Li, 3D-printed repeating re-entrant topography to achieve on-demand wettability and separation, ACS Appl. Mater. Interf. 12 (31) (2020) 35725–35730.
[25] Y. Liu, H. Zhang, P. Wang, Z.Y. He, G.N. Dong, 3D-printed bionic superhydrophobic surface with petal-like microstructures for droplet manipulation, oil-water separation, and drag reduction, Mater. Des. 219 (2022), 110765.
[26] Q. Yin, Q. Guo, Z.L. Wang, Y.Q. Chen, H.G. Duan, P. Cheng, 3D-printed bioinspired Cassie-Baxter wettability for controllable microdroplet manipulation, ACS Appl. Mater. Interf. 13 (1) (2020) 1979–1987.
[27] L. Han, C. Chen, L.G. Shen, H.J. Lin, B.S. Li, Z.Y. Huang, Y.C. Xu, R.J. Li, H.C. Hong, Novel membranes with extremely high permeability fabricated by 3D printing and nickel coating for oil/water separation, J. Mater. Chem. A 10 (22) (2022) 12055–12061.
[28] L. Han, L.G. Shen, H.J. Lin, Z.Y. Huang, Y.C. Xu, R.J. Li, B.S. Li, C. Chen, W. Yu, J. H. Teng, 3D printing titanium dioxide-acrylonitrile-butadiene-styrene (TiO_2-ABS) composite membrane for efficient oil/water separation, Chemosphere 315 (2023), 137791.
[29] Y.G. Guo, B.P. Luo, X.C. Wang, S.H. Liu, T. Geng, Wettability control and oil/water separation performance of 3D-printed porous materials, J. Appl. Polym. Sci. 139 (5) (2022), 51570.
[30] L. Han, L.G. Shen, H.J. Lin, T.H. Cheng, J.M. Wen, Q.N. Zeng, Y.C. Xu, R.J. Li, M. J. Zhang, H.C. Hong, C.Y. Tang, Z.L. Wang, Three dimension-printed membrane for ultrafast oil/water separation as driven by gravitation, Nano Energy 111 (2023), 108351.
[31] Z.P. Jin, H. Mei, Y.K. Yan, L.K. Pan, H.X. Liu, S.S. Xiao, L.F. Cheng, 3D-printed controllable gradient pore superwetting structures for high temperature efficient oil-water separation, J. Mater. 7 (1) (2021) 8–18.
[32] J. Lv, Z.J. Gong, Z.K. He, J. Yang, Y.Q. Chen, C.Y. Tang, Y. Liu, M.K. Fan, W.M. Lau, 3D printing of a mechanically durable superhydrophobic porous membrane for oil-water separation, J. Mater. Chem. A 5 (24) (2017) 12435–12444.
[33] Z.K. He, Y.Q. Chen, J. Yang, C.Y. Tang, J. Lv, Y. Liu, J. Mei, W.M. Lau, D. Hui, Fabrication of Polydimethylsiloxane films with special surface wettability by 3D printing, Compos. Part. B-Eng. 129 (2017) 58–65.
[34] X.P. Li, H.T. Shan, W. Zhang, B.A. Li, 3D printed robust superhydrophilic and underwater superoleophobic composite membrane for high efficient oil/water separation, Sep. Purif. Technol. 237 (2020), 116324.
[35] P. Ghosal, B. Gupta, R.S. Ambekar, M.M. Rahman, P.M. Ajayan, N. Aich, A. K. Gupta, C.S. Tiwary, 3D printed materials in water treatment applications, Adv. Sustain. Syst. 6 (3) (2022), 2100282.
[36] L.D. Tijing, J.R.C. Dizon, I. Ibrahim, A.R.N. Nisay, H.K. Shon, R.C. Advincula, 3D printing for membrane separation, desalination and water treatment, Appl. Mater. Today 18 (2020), 100486.